High Interaction Regime Lockhart-Martinelli Model for Pressure Drop in Trickle-Bed Reactors

Dario Pinna and Enrico Tronconi
Dipartimento di Chimica Industriale e Ingegneria Chimica, Politecnico di Milano, 20123 Milano, Italy

Lorenzo Tagliabue
Snamprogetti S.p.A., Research Laboratories, 20097 S. Donato Milanese, Italy

Pressure drop and liquid saturation in a cold model representative of trickle-bed reactors operating in the high interaction regime were measured using air and water at atmospheric pressure. Five different packings similar in shape and dimension to typical industrial catalysts (cylindrical pellets, raschig rings, extrudates) were tested, covering a wide range of geometric characteristics. The adequacy of the most recent literature correlations for pressure drop in trickle-bed reactors was checked. The best predictions are provided by an empirical correlation based on the Lockhart-Martinelli parameters. A new model of similar accuracy was derived, which provides a theoretical basis for the successful application of the Lockhart-Martinelli approach.

Introduction

Trickle-bed reactors have been mainly developed for the refining industry (Satterfield and Way, 1972; Satterfield, 1975; Paraskos et al., 1975, Charpentier, 1976; Dudukovic and Mills, 1986). Indeed, recent studies have shown that this technology can also be extended to many other catalytic processes of considerable industrial interest, particularly to those involving very exothermic reactions. Examples are the methanol synthesis (Galtier et al., 1986; Pass et al., 1990; Kodra and Levec, 1991; Tjandra et al., 1993; Cybulski et al., 1993; Cybulski, 1994) and the synthesis of hydrocarbons from CO and H_2 (Audibert et al., 1983; Chaumette, 1996). Traditionally such processes have been carried out in gas-solid fixed bed reactors equipped with complex cooling systems (Ullmann's Encyclopedia, 1990) and operating at low conversions per-pass with high recycle rates.

On the contrary, in trickle-bed reactors an additional inert liquid is introduced to absorb the heat released by the reaction (Satterfield and Way, 1972) and to improve the otherwise difficult temperature control. In the case of equilibrium-limited reactions the conversion per-pass can be significantly enhanced, while the recycle of unreacted gas is drastically reduced.

For this application a further alternative to trickle-bed reactors is represented by slurry reactors. Even if a slurry reactor leads to a better catalyst utilization, a trickle-bed reactor may be preferred because it features higher productivities per unit reactor volume (Kodra and Levec, 1991) and avoids potential catalyst handling problems.

The trickle-bed reactor solution requires however circulation of high flow rates of liquid to remove the reaction heat: this leads to operate the gas/liquid/solid reactor in the so-called *high interaction regime* (Benkird et al. 1997; Tosun 1984), which is characterized by considerable energy dissipation, that is high pressure-drops. Thus, the accurate prediction of pressure drop is important in design and optimization of trickle-bed reactors-based synthesis units.

In order to verify the applicability of existing correlations for pressure-drop calculation to the peculiar conditions required by the described processes, an experimental setup has been built and operated at Snamprogetti to collect pressure drop and liquid saturation measurements in a cold model of a trickle-bed reactor.

Survey of Literature Correlations

A number of mathematical models have been proposed in the literature to predict pressure-drop and liquid saturation in trickle-bed reactors. Still, since the present main application of trickle-bed reactors is the hydrotreating of oil fractions, most of the published works are relative to the *low*

Correspondence concerning this article should be addressed to E. Tronconi.

interaction fluid-dynamic regime, which is typical of these processes.

In this work the most recent correlations for predicting pressure-drop in the high interaction regime are evaluated (Pinna, 1999). These are summarized in Table 1.

Most of the examined models are empirical correlations of some dimensionless groups, such as a friction factor, the Reynolds, the Weber and the Lockhart-Martinelli numbers (Wammes et al., 1991).

The phenomenological models, on the other hand, are developed on the basis of force balances, acounting for friction at the interfaces.

The class of the empirical models includes the correlations by Specchia and Baldi (1977), Tosun (1984), Larachi et al. (1991), Bensetiti et al. (1997), whereas the models proposed by Yang et al. (1993), Benkird et al. (1997) and Al-Dahhan et al. (1998) are semi-theoretical ones.

The model by Specchia and Baldi (1977) is derived from the one proposed by Turpin and Huntington (1967). The pressure-drop is expressed in terms of a friction factor f_{LG}, which is assumed to be a function of the dimensionless number ζ (a combination of the liquid and the gas Reynolds numbers). The pressure-drop is dependent upon the physical properties of the fluids also through the parameter Ψ, previously introduced by Charpentier and Favier (1975).

Tosun (1984) has proposed a correlation between the Lockhart-Martinelli dimensionless groups (Lockhart and Martinelli, 1949)

$$\chi = \left[\frac{\left(\frac{\Delta P}{Z}\right)_L}{\left(\frac{\Delta P}{Z}\right)_G} \right]^{1/2} \qquad \phi = \left[\frac{\left(\frac{\Delta P}{Z}\right)_{LG}}{\left(\frac{\Delta P}{Z}\right)_L} \right]^{1/2} \tag{1}$$

The definition of the two parameters involves the estimates of single-phase pressure-drops across the packing (subscript L and G) and the measurement of the pressure-drop in two-phase flow (subscript LG). The single-phase

Table 1. Examined Literature Model for Pressure-Drop and Liquid Saturation in TBRs

Model	Functional Expression	Notes
Specchia and Baldi (1977)	$\ln f_{LG} = 7.82 - 1.30 \ln\left(\frac{\zeta}{\psi^{1.1}}\right) + 0.0573\left[\ln\left(\frac{\zeta}{\psi^{1.1}}\right)\right]^2$	Turpin and Huntington-type model.
Tosun (1984)	$\phi = 1 + \frac{1}{\chi} + \frac{1.424}{\chi^{0.576}}$	Lockhart and Martinelli-type model.
Ellman et al. (1988)	$f_{LG} = 6.96 \cdot (\chi_G \xi)^{-2} + 5327 \cdot (\chi_G \xi)^{-1.5}$	Developed with a step-wise method.
Larachi et al. (1991)	$f_{LG} = \frac{1}{\kappa^{1.5}}(31.3 + \frac{17.3}{\kappa^{0.5}})$	Developed for high pressures.
Yang et al. (1993)	$\beta = \frac{0.49 \cdot \frac{u_G}{u_L} + 1}{\frac{u_G}{u_L} + 1}$	Developed from the *drift flux* concept. It takes into account only the superficial velocity of the fluids.
Benkird et al. (1997) (*Mod. A*)	$\left(\frac{\Delta P}{Z}\right)_{LG} = \left(\frac{2.31}{\epsilon\beta}\right)^{2.5} \frac{a_{LS} \cdot \rho_L \cdot u_L^{1.5} \cdot \mu_L^{0.5}}{d_P^{0.5}}$	Developed from force balances: it does not take into account the friction at the liquid-gas interface. It needs a model for liquid saturation.
Benkird et al. (1997) (*Mod. B*)	$\left(\frac{\Delta P}{Z}\right)_{LG} = \left(\frac{1}{\epsilon\beta}\right)^3 \left(150 \cdot \frac{a_{LS}}{36} \mu_L u_L + 1.75 \cdot \frac{a_{LS}}{6} \rho_L u_L^2\right)$	Ergun-type model. It does not take into account the friction at the liquid-gas interface. It needs a model for liquid saturation.
Bensetiti et al. (1997)		Neural network model for β developed on a wide data bank.
Al-Dahhan et al. (1998)	$\Psi_L = 1 + \frac{\rho_G}{\rho_L}(\Psi_G - 1)$ $\Psi_G = \left(\frac{\epsilon}{\epsilon_G}\right)^3 \left[150 \cdot \frac{Re_G - f_v \epsilon_G Re_i}{Ga_G} + 1.75 \cdot \frac{(Re_G - f_v \epsilon_G Re_i)^2}{Ga_G}\right]$ $\Psi_L = \left(\frac{\epsilon}{\epsilon_L}\right)^3 \left[150 \cdot \frac{Re_L}{Ga_L} + 1.75 \cdot \frac{Re_L^2}{Ga_L}\right] + f_s \frac{\epsilon_G}{\epsilon_L}\left(1 - \frac{\rho_G}{\rho_L} - \Psi_L\right)$ $f_s = -4.4 \times 10^{-2} \cdot Re_G^{0.15} \cdot Re_L^{0.15}$ $f_v = -2.3 \cdot \mathrm{Re}_G^{0.05} \cdot \mathrm{Re}_L^{-0.05}$	Developed from force balances, assuming that the friction at liquid-solid and liquid-gas interfaces can be represented by an Ergun-like expression. The parameters are estimated by application in the *low* interaction regime at high pressure.

pressure-drops can be calculated using the Ergun equation (Bird et al., 1960).

The set of experiments used by Tosun to derive the correlation covered liquids and gases of various nature (air/water; He/50% glycerine in water; He/(32% glycerine + 30% ethanol + 38% water); He/80% metanol in water; air/80% methanol in water; air/28% glycerine in water), but only *one* type of packing (glass beads with an average diameter of 1.99 mm and a void fraction of 0.344).

Ellman et al. (1988) correlated the friction factor f_{LG} to the modified Lockart and Martinelli gas number X_G and to a dimensionless number ζ, function of the liquid Reynolds and Weber numbers. The mathematical expression of the correlation is the result of a step-wise regression method applied to a data bank covering a wide range of liquid and gas flow rates.

Also the model by Larachi et al. (1991) allows calculating the pressure-drop in terms of a friction factor f_{LG} as a function of the dimensionless number κ, which is a suitable empirical combination of the liquid Reynolds and Weber numbers. The correlation has been developed specifically at high pressure, a very desirable condition when applied to the methanol and hydrocarbon synthesis from CO and H_2. In a recent work Benkird et al. (1997) have proposed two phenomenological models herein presented as model A and model B) to predict pressure-drop and liquid saturation in a trickle-bed reactor in the high interaction regime. The basic hypothesis is that the solid is entirely wetted by the liquid. In such a system all the pressure-drop is supposed to be due to the friction at the liquid-solid interface and the effect of the gas phase is confined to the reduction of the available liquid flow section.

Model A and model B differ only in the way of modeling the liquid-solid interaction. The former postulates that the shear at the interface is the same one produced by a liquid flow over a flat plate. The latter uses an Ergun-like approach. In both models the real velocity of the liquid is taken into account, so that in the final expressions the liquid saturation β is included.

The correlation for liquid saturation adopted by the authors is the *drift flux* one, previously introduced by Yang et al. (1993). Yet it can be noticed that according to the *drift flux* model the liquid saturation β is a function of the ratio of the superficial velocities of the fluid (u_G/u_L) only and does not depend upon the fluid properties nor upon the geometric characteristics of the packings. In addition at high values of u_G/u_L β is expected to reach an asymptote of 49%, while for intermediate values of u_G/u_L the predicted liquid saturation remains between 100% and 49%, which has no theoretical justification.

The just described limits of the *drift flux* model may lead to unreliable predictions of pressure-drop. Accordingly in this work the *drift flux* model has been replaced in the expressions of model A and B for pressure-drop by another allegedly more reliable liquid saturation model. The selected correlation is the multilayer artificial neural network model by Bensetiti et al. (1997). The adaptive parameters of the network were estimated by fitting the model to over 2600 measurements collected by various authors between 1960 and 1997. Even if developed to be used in upflow, this correlation can be applied to the present set of experiments since in the high interaction regime the direction of the flow does not significantly affect the liquid saturation (Benkird et al., 1997; Lamine et al., 1996).

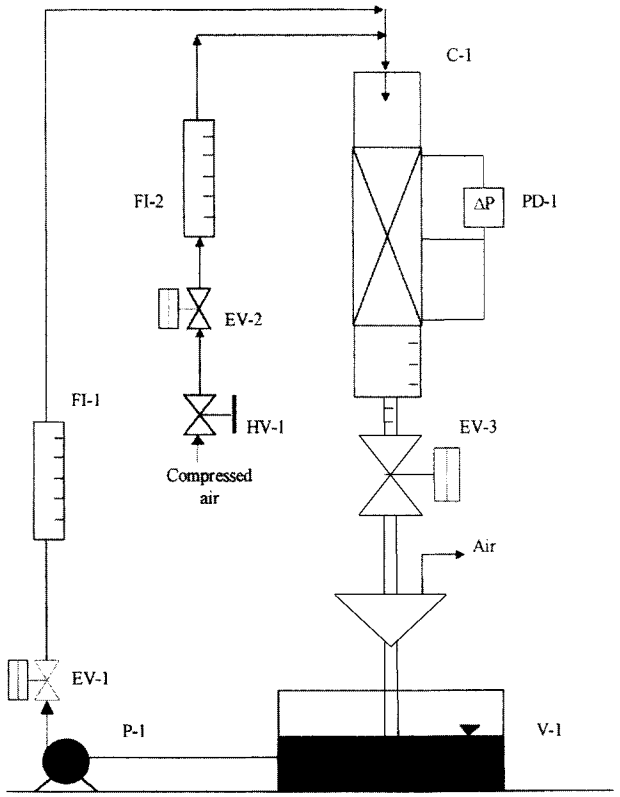

Figure 1. Cold model.

The last correlation analyzed is the one presented by Al-Dahhan et al. (1998). Although specifically developed for the low interaction regime, this model has been herein considered because of its phenomenological nature. The model is based on the assumption that the liquid flows as a film on the solid, completely wetting it, and that the gas flows in a central core: the friction both at the liquid-solid and at the liquid-gas interfaces is considered and estimated according to the Ergun equation. As discussed below, this hypothesis can be supposed to hold for a high interaction regime, too. The model was fitted to a set of data collected at high pressure, where the authors found a non negligible interaction between the gas and the liquid phases. The final form of the model is a nonlinear algebraic system to be solved in the dimensionless pressure-drops (Ψ_L and Ψ_G) and liquid holdup (ϵ_L).

Experimental

The core of the apparatus (Figure 1) used in this work is the plexiglas column C-1 (2 m in height, ID 10 cm). The liquid (water) and the gas (air) flow cocurrently downflow through a packed bed.

The liquid is circulated by the peripheral pump P-1 (maximum flow rate = 3 m^3/h, max. head = 3 bar).

The liquid flow rate is regulated by modifying the impeller speed through an inverter and is measured by the rotameter FI-1. The gas comes from the compressed air line: it is con-

Table 2. Fluid Properties

ρ_L	kg/m^3	1,000
ρ_G	kg/m^3	1.20–2.38
μ_L	kg/m/s	0.001
μ_G	kg/m/s	1.18×10^{-5}
σ_L	kg/s^2	0.072

trolled by the manual valve HV-1 and measured by the rotameter FI-2.

To convert the flow rate from volumetric to massive, a density of 1.19 kg/m^3 is assumed for the air.

Eventually the gas-flow rate G is corrected with the following expression, to take into account the real pressure of the air in the instrument (Perry and Green, 1984)

$$G_{\text{real}} = G \cdot \sqrt{\frac{P_{\text{out}} + \left(\frac{\Delta P}{Z}\right)_{\text{meas}} \cdot Z}{P_{\text{ref}}}} \tag{2}$$

with $P_{\text{OUT}} = P_{\text{ref}} = 1.013$ bar.

Before entering the top of the column, water and air are mixed together in a Venturi-type ejector. The uniformity of the flow over the packed bed is assured by a shower 20 cm above the packing.

Pressure-drop measurements across the packing are collected by means of the DP-cell PD-1. Two different packing heights have been used (0.5 or 1 m) to keep the total pressure-drop below 1 bar and prevent structural damage to the column.

Liquid saturation measurements have been carried out too, by using the volumetric method (Yang et al. 1993; Benkird et al., 1997), due to its simplicity and reliability. For this purpose, two electrovalves EV-1 and EV-2, installed upstream to both the gas and the liquid rotameters, shut off the inlet streams. A third electrovalve EV-3 is placed at the bottom of the column.

The ratio of the liquid drained from the column to the void volume of the packing gives the dynamic liquid saturation.

The liquid retained in the interstices between the packing particles after the bed has been drained is taken into account by additing a static term. This *static liquid saturation* is estimated according to the empirical model (Saez and Carbonell, 1985)

$$\beta_{\text{stat}} = \frac{1}{\epsilon \cdot (20 + 0.9 E\ddot{o}^*)} \tag{3}$$

where $E\ddot{o}^*$ is the Eötvos number.

The properties of the fluids and of the packings are sumarized in Table 2 and Table 3. In all experiments the D_t/d_p ratio was greater than or equal to 10, ruling out wall effects (Mears, 1971). It should be noted that the particle shapes (cylindrical pellets and raschig rings) are typical of many widely used catalysts. The wide range of void fractions and dimensions associated with the tested packings is also worthy of note.

Table 3. Properties of the Tested Packings

Type	OD/ID/H (mm)	d_p (mm)	ϵ	$\phi_s = d_p/d_V$	d_s (mm)	Material
Cylindrical pellets	6/–/6	6.46	0.378	0.87	7.91	PVC
Cylindrical pellets	10/–/10	10.50	0.397	0.87	12.85	PVC
Raschig rings	9/6/9	4.92	0.576	0.51	13.35	Acrylic fiber
Raschig rigs	15/9/15	7.46	0.650	0.51	20.51	Acrylic fiber

Table 4. Number of Collected Measurements

Type	β Measurements	$\Delta P/Z$ Measurements
Pellet 6×6	110	110
Pellet 10×10	125	134
Raschig 9×6	66	113
Raschig 15×9	137	137
Total	438	494

All the experiments have been carried out at atmospheric pressure and room temperature. A large spectrum of high liquid and gas specific flow rates has been covered: L = 14.73–73.65 kg/m^2/s and G = 0.86–3.45 kg/m^2/s.

The resulting data bank consists of about 500 pressure-drop and 440 liquid saturation measurements (Table 4).

Results and Discussion

Analysis of experimental pressure-drop and liquid saturation data

The hydrodynamic regime of the system is determined by locating our data on the flow map of Morsi et al. (1984): all the experimental points lay in the *pulsing* region, corresponding to the high interaction regime over the whole field of flow rates.

From the experimental measurements it can be observed that the pressure drop increases with increasing liquid and gas specific flow rates, whereas it decreases on increasing the particle size and the bed void fraction. Also, the liquid saturation increases for increasing L and for decreasing G, and its dependency on particle characterstics is weak.

As a first step in data reduction, we attempted to plot all the pressure-drop measurements in a single graph, using the Lockhart-Martinelli parameters χ and ϕ. The single-phase pressure-drops, required for computation of χ and ϕ, were estimated according to the classic Ergun equation (Bird et al., 1960).

In Figure 2 the entire data bank is represented according to the Lockhart-Martinelli coordinates.

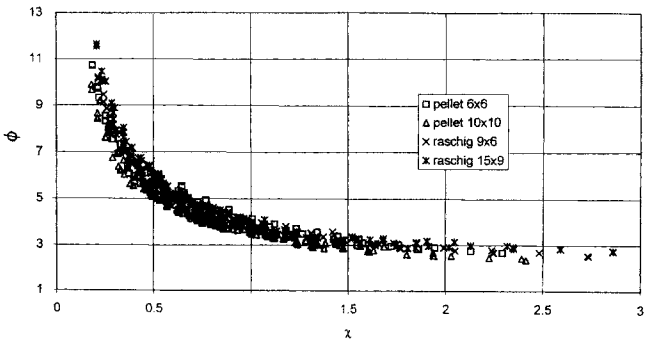

Figure 2. Experimental values of pressure-drop.

Table 5. Experimental Ranges: This Work vs. Literature Correlations

		This Work	Specchia and Baldi	Tosun	Ellman et al.	Larachi et al.	Benkird et al.	Bensetiti et al.	Al-Dahhan et al.
L	kg/m^2/s	14.73–73.65		3–30	0.5–105	1.8–24.5	10–105		0.42–4.1
G	kg/m^2/s	0.86–3.450		0.0005–1	0.01–10	0.003–2.2	0.01–2.51		0.0064–4.03
d_p	mm	4.92–10.5	3–22	1.9		1.4–2	1.4–6.7		1.1–1.99 (est.)
d_s	mm	7.91–20.50			1.16–3.06	1.4–2			1.1–2.82 (est.)
d_v	mm	7.43–12.07				1.4–2		0.46–25.4	1.1–2.51 (est.)
ϵ	—	0.38–0.65		0.344	0.273–0.489	0.35–0.38	0.35–0.489	0.30–0.47	
u_L	cm/s	1.47–7.36	0.16–2.5					0.046–2.54	0.042–0.41
u_G	cm/s	57.0–315.3	1.1–246					0.004–203	1–11.7

On the basis of the data reported in Figure 2, two important remarks apply:

- There is an essentially unique correlation between χ and ϕ which does not seem to be significantly dependent upon the geometric characteristics of the packing;
- The experimental points set in a somehow hyperbolic form, ϕ approaching infinity and one as χ goes to zero and to infinity, respectively, in line with the expected asymptotic behavior of the L-M correlation.

Test of literature correlations

Table 5 presents a comparison between the ranges of the variables covered in this work and the ones for which each literature model was developed: it is noteworthy that, when applied to the present data, every correlation has been employed outside its own experimental field, and that the most extreme variables are the packing characteristics (void fraction and particle dimension).

In view of the results of Figure 2, all the literature correlations have been visually tested by expressing the pressure drop estimated by each model in terms of the Lockhart-Martinelli parameters, and comparing them to the experimental ones.

Furthermore, to quantify the adequacy of each model, two error indexes have been built: *AEa* = average modulus of the difference between the calculated and measured pressure drop

(Absolute Error average), (bar/m)

$$= \underset{i}{\text{average}} \left| \left(\frac{\Delta P}{Z}\right)_{i,\text{calc}} - \left(\frac{\Delta P}{Z}\right)_{i,\text{exp}} \right| \tag{4}$$

REa = average difference between the calculated and the measured pressure-drop, relative to the latter

(Relative Error, average),

$$= \underset{i}{\text{average}} \left[\frac{\left(\frac{\Delta P}{Z}\right)_{i,\text{calc}} - \left(\frac{\Delta P}{Z}\right)_{i,\text{exp}}}{\left(\frac{\Delta P}{Z}\right)_{i,\text{exp}}} \right] \tag{5}$$

The results of the analysis are summarized in Table 6 and 7.

The correlation which best fits the *whole* data bank is the one proposed by Tosun (1984), the corresponding *AEa* indexes being much lower than the ones computed for all the other correlations.

No model but the one by Tosun leads to accurate pressure-drop predictions for *all* the examined packings. Some models (Specchia and Baldi, Benkird et al. A coupled with Bensetiti et al.) give satisfactory results when applied to the pellet beds, but result in poor predictions for ring packings. The other correlations proved unreliable over the entire set of measurements.

It is noticeable that, according to the *AEa* indexes, the second best model is the one by Al-Dahhan, although it was developed for trickle flow.

The lack of accuracy of most correlations is likely due to the fact that every model is somewhat extrapolated with respect to one or more variables: yet the model by Tosun, which is also extrapolated, is quite effective in reproducing the measured pressure-drop, as apparent by inspection of Figure 3. This seems to be a consequence of adopting a Lockhart-Martinelli approach.

Also the model by Al-Dahhan et al., even if far extrapolated, results in a quasi-unique correspondence between the Lockhart-Martinelli parameters (Figure 4). The scatter of some calculated points may be due to numerical sensitivity of the model solutions.

Table 6. Test of Literature Correlations: *AEa* Indexes

AEa	Pellet 6×6	Pellet 10×10	Raschig 9×6	Raschig 15×9	Avg.
$\Delta P/Z$ average (bar/m)	~1	~0.8	~0.3	~0.15	
Specchia and Baldi	0.26	0.18	0.62	0.25	0.32
Tosun	0.15	0.02	0.04	0.03	0.06
Ellman et al.	0.67	0.27	0.07	0.06	0.25
Larachi et al.	1.00	0.46	0.26	0.11	0.44
Benkird et al. A	0.79	0.36	0.16	0.07	0.33
Benkird et al. B	0.59	0.23	0.14	0.06	0.24
Benkird et al. A & Bensetiti et al.	0.20	0.35	4.39	11.32	4.29
Benkird et al. B & Bensetiti et al.	0.92	0.20	11.63	32.58	11.96
Al-Dahhan et al.	0.31	0.17	0.12	0.06	0.16

Table 7. Test of Literature Correlations: *REa* Indexes

REa	Pellet 6×6	Pellet 10×10	Raschig 9×6	Raschig 15×9	Avg.
Specchia and Baldi	22.6%	41.1%	220.1%	283.3%	132.6%
Tosun	−15.4%	−1.9%	−17.0%	−25.0%	−14.8%
Ellman et al.	−61.8%	−51.7%	14.3%	−48.9%	−38.1%
Larachi et al.	−90.6%	−91.0%	−92.3%	−92.7%	−91.7%
Benkird et al. A	−72.3%	−69.8%	−57.7%	−59.5%	−64.7%
Benkird et al. B	−54.6%	−42.4%	−51.6%	−49.8%	−49.3%
Benkird et al. A & Benesetiti et al.	−15.6%	−69.4%	1575.5%	1512.2%	757.5%
Benkird et al. B & Benesetiti et al.	71.3%	−42.3%	3947.7%	4127.5%	2052.1%
Al-Dahhan et al.	−22.6%	−20.9%	−17.2	−29.9%	−22.9%

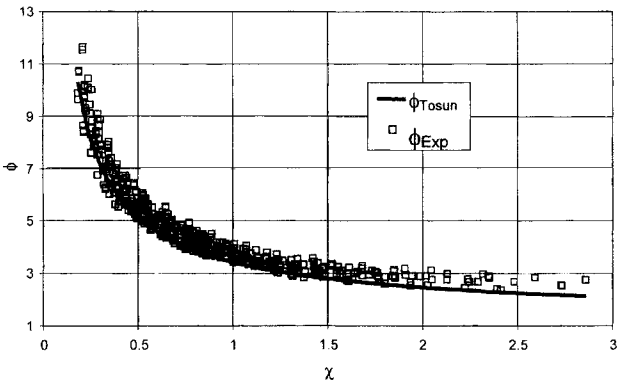

Figure 3. Model by Tosun (1984): comparison with experimental data.

On the contrary the other models do not involve a direct correlation between the two Lockhart-Martinelli parameters thus generally yielding incorrect predictions. Figure 5 reports, as an example, a comparison between the experimental values of ϕ and the ones calculated according to the Specchia and Baldi model: the correlation is very good for the pellets but is rather inadequate for the raschig rings.

Theoretical basis for the Lockhart-Martinelli correlation

It has been pointed out that the best literature pressure-drop model is the one presented by Tosun (1984). Still, this correlation is empirical, and thus no further extrapolation to other packing types and flow conditions could be in principle recommended.

Also the Al-Dahhan model leads to good results, considering that it was developed for a different flow regime.

Moving from these considerations, in this section a theoretical model for pressure-drop and liquid saturation in trickle-bed reactor is developed, which rationalizes the observed direct correlation between the Lockhart-Martinelli parameters.

For this purpose a procedure similar to the one proposed by Taitel and Dukler (1976) for stratified two-phase pipe flow has been adopted and modified to apply to the specific fluid-dynamic system (Pinna, 1999).

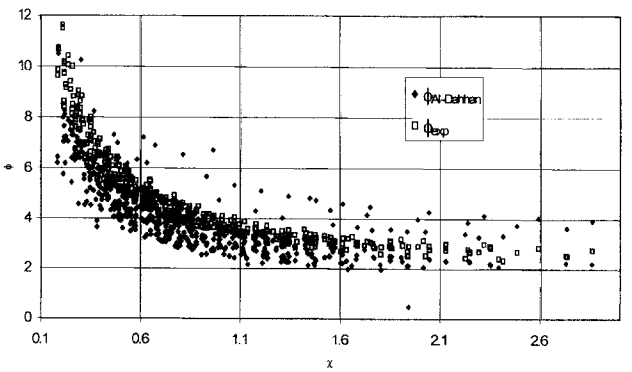

Figure 4. Model by Al-Dahhan et al. (1998): comparison with experimental data.

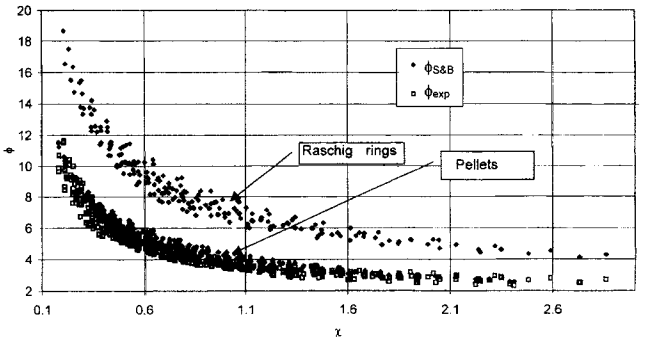

Figure 5. Model by Specchia and Baldi (1977): comparison with experimental data.

Following Al-Dahhan et al. (1998) and Benkird et al. (1997), we postulate that the solid surface of the packing is completely wetted by the liquid. In addition the interaction between the gas and the liquid phases is taken into account, whereas inertial forces and surface tension effects are neglected, in view of the flow conditions prevailing in the high interaction regime.

Also, the gravity term is not accounted for, being negligible in the investigated regime (Benkird et al., 1997; Lamine et al., 1996).

Eventually, following Saez and Carbonell (1985), Al-Dahhan et al. (1998), Holub et al. (1992, 1993), capillary pressure is supposed to be negligible too.

In order to write the momentum balance equations on the liquid and the gas phases in a dimensionless form, the geometry illustrated in Figure 6 is assumed: the liquid and the gas are supposed to flow through a channel, representative of the void interstices between the solid particles. The channel has an equivalent diameter D_H and forms an angle θ with the vertical axis.

The flow is assumed to be annular, the gas moving through a coaxial channel of diameter δ surrounded by the liquid.

Notably, the assumption of separated flow for the high interaction regime is consistent with the boundary layer model described by Benkird et al. (1997) and is reported by Rode et al. (1994) to be representative of high interaction regime flows.

By considering the effective flow sections of the liquid and the gas, by eliminating the two-phase pressure-drop between the momentum balances and by introducing dimensionless parameters, we get two equations that correlate the two-phase pressure-drop, the single-phase pressure-drops and the liquid saturation.

Upon introducing the two Lockhart-Martinelli dimensionless groups (Eq. 1), the model turns out to be

$$\chi^2 = \alpha \cdot \frac{(1-\tilde{\delta})^{0.2} \cdot (1-\tilde{\delta}^2)^{1.8}}{\tilde{\delta}^{4.8}} \tag{6}$$

$$\phi^2 = \frac{1}{(1-\tilde{\delta})^{0.2} \cdot (1-\tilde{\delta}^2)^{1.8}} \tag{7}$$

with the liquid saturation given by

$$\beta = 1 - \tilde{\delta}^2 \tag{8}$$

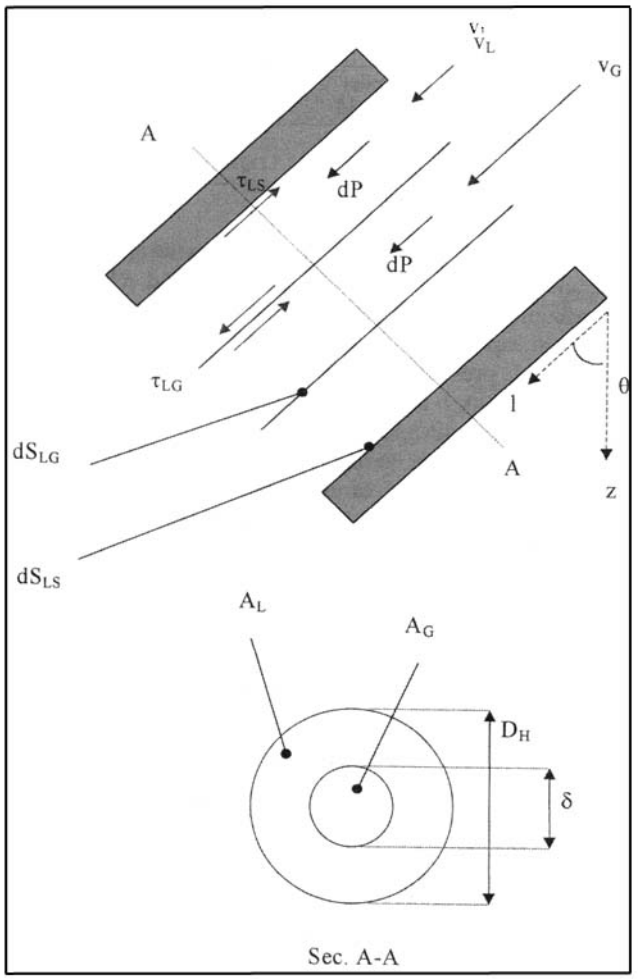

Figure 6. Geometry of the flow system.

The proposed model contains only the adaptive parameter

$$\alpha = \frac{f_l}{f_g} \tag{9}$$

regarded as a constant.

For the details of the derivation see the Appendix.

Equation 6 allows to calculate $\bar{\delta}$ from χ and thus the liquid saturation, via Eq. 8.

Once $\bar{\delta}$ is known, the dimensionless pressure-drop ϕ can be obtained from Eq. 7.

Notably, all the information about the geometry of the packing (that is, tortuosity, equivalent diameter of the channel) is not directly considered in the final form of the model, Eqs. 6 and 7. Indeed, such geometrical parameters are implicitly taken into account in the evaluation of the single-phase pressure-drops, such as on the basis of the Ergun equation, possibly including also different E_1 and E_2 constants for various particle shapes (Charpentier, 1978). Thus, for example, the two-phase pressure-drop is dependent upon the equivalent diameter of the sphere having the same surface to volume ratio as the particle (d_p) and upon the bed void fraction (ϵ), even though such dependencies are not explicity in Eqs. 6 and 7.

For low ratios of L/G (that is, low values of χ) Eqs. 6 and 7 predict that $\bar{\delta}$ and ϕ approach one and infinity respectively: in these conditions the liquid saturation goes to zero. For high ratios of L/G (that is, high values of χ) the model estimates a liquid saturation near to one and a pressure-drop close to the one evaluated for the liquid. The physical consistency of the model is then assured, regardless of the value of α and of the equations used to evaluate the single-phase pressure-drops.

To estimate the adaptive parameter α, Eq. 6 has been fitted to the liquid saturation measurements by minimizing the function

$$F(\alpha) = \sum_{i=1}^{N} \left(\beta_{i,\text{calc}} - \beta_{i,\text{exp}} \right)^2 \tag{10}$$

The best fit was found (Buzzi-Ferraris, 1998) with a value of

$$\alpha = 3.56 \pm 0.302 \quad (\text{confidence} = 95\%)$$

Once α is known, Eq. 7 becomes a purely predictive model to estimate ϕ, which does not include any other adaptive parameter.

A sensitivity analysis of the model to variations of the value of α indicates that predictions of β and ϕ are not strongly sensitive to an oscillation of α of about 42%, leading to relative variations less than 30%.

Test of the new model and comparison with the correlation of Tosun

Equations 6 and 7 provide a theoretical justification of the experimentally observed unique correlation between the two Lockhart-Martinelli parameters. Figure 7 shows a satisfactory agreement between the values of ϕ calculated from the model and the experimental ones: considering that the estimate of the single parameter α was derived from a regression on liquid saturation data only, the results seem acceptable.

For high values of χ though, the model tends to slightly understimate the experimental pressure-drop. In these conditions, corresponding to high L/G ratios, formation of bubbles may occur, the geometry previously assumed thus becoming a maybe too simple schematization of the real flow pattern.

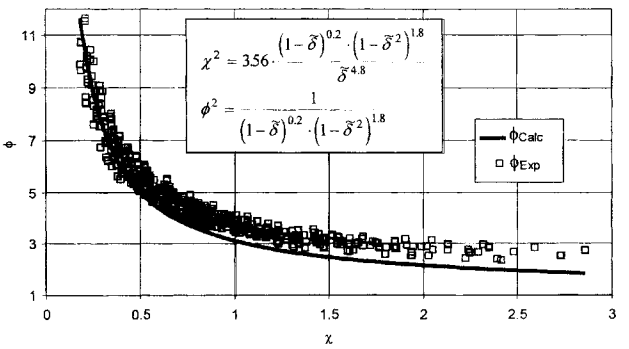

Figure 7. Proposed model, Eqs. 6–7: prediction of $\Delta P/Z$ and comparison with present data.

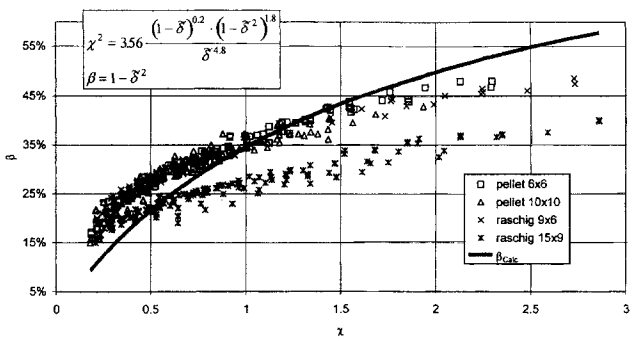

Figure 8. Proposed model, Eqs. 6–7: prediction of β and comparison with present data.

On the other hand Figure 8 presents a comparison between the experimental values of liquid saturation and the ones calculated from Eq. 6. Actually, while according to Eq. 6 liquid saturation should be a function of χ alone, only three of the four packings experimentally show such a direct dependency, the values of β measured over the 15×9 raschig bed being a little lower than the ones collected over the other packings, at the same value of χ. Furthermore, the model turns less accurate at the very extremes of the abscissa. For low χ, this inaccuracy could be explained in view of the results reported by Charpentier et al. (1968): when the liquid flow rate is low with respect to the gas, part of the liquid could be transported in the gas channel in the form of small drops (mist). Since the liquid saturation relative to these droplets cannot be computed, given the assumed geometry (see Figure 6), the model tends to underpredict the real liquid saturation. On the contrary, for very high χ, correspondings to high values of L/G, the deviation can be explained by formation of bubbles, as mentioned.

Still the comparison between calculated and measured liquid saturation results seems acceptable for intermediate values of χ.

In Table 8 and Table 9 the *AEa* and *REa* indexes are given for the proposed model and for the one by Tosun. The predictions of ϕ calculated from the two models are very close to the measured ones for each packing type, as indicated by the low values of *AEa*. Since the values of *REa* are negative, both models tend to slightly underestimate the pressure drop. Actually, the model by Tosun is slightly superior, but it must be considered that the correlation of Tosun includes *two* adaptive aprameters which were estimated by fitting *pressure-drop* measurements, while the present model contains only *one* parameter, whose estimate has been obtained by fitting *liquid saturation* measurements.

A graphic comparison between the two correlations (Figure 9) demonstrates that the models exhibit a similar behavior, the relative differences on ϕ ranging between −30% and 10%, and justifies the similarity of the *AEa* and *REa* indexes. Accordingly, considering that the Tosun correlation was derived from experiments collected with several types of fluids, and that the presented new model is a theoretical one, we propose that Eqs. 6 and 7 could be applied tentatively also to fluids other than air and water.

Table 8. Comparison Between the New Model and the One by Tosun: *AEa* Indexes

AEa	Pellet 6×6	Pellet 10×10	Raschig 9×6	Raschig 15×9	Avg.
$\Delta P/Z$ avg. (bar/m)	~1	~0.8	~0.3	~0.15	
This work	0.25	0.08	0.06	0.04	0.10
Tosun	0.15	0.02	0.04	0.03	0.06

Table 9. Comparison Between the New Model and the One by Tosun: *REa* Indexes

REa	Pellet 6×6	Pellet 10×10	Raschig 9×6	Raschig 15×9	Avg.
This work	−23.6%	−10.3%	−25.2%	−33.5%	−23.1%
Tosun	−15.4%	−1.9%	−17.0%	−25.0%	−14.8%

In order to further verify the reliability of the proposed model, an additional set of experiments has been eventually carried out at even higher liquid and gas flow rates, using a packing of alumina extrudates with an equivalent diameter of 4.99 mm and a void fraction of 0.476. Pressure-drop predictions turned out to be reasonably good (Figure 10): the average relative error on pressure-drop was found to be −3.5% and the average absolute error 0.125 bar/m (Table 10).

Conclusions

A pressure-drop data bank has been built, which covers a wide range of operating conditions and of packing characteristics. It has been shown that all the pressure-drop measurements can be synthetically represented in terms of the Lockhart-Martinelli dimensionless parameters χ and ϕ. A related result is that the only literature correlation which provided satisfactory predictions for the whole set of experiments was the empirical correlation between χ and ϕ proposed by Tosun (1984). This model was developed by fitting pressure-drop measurements collected with *several* couples of liquids and gases but over just one packing. Yet, amidst the tested literature correlations, the model of Tosun is the only one that leads to accurate predictions of pressure-drop for *all the packings* examined in this work.

We have derived a theoretical explanation of the observed correlation between χ and ϕ, based on simple momentum balances. The analysis includes a single adpative parameter α, which has been estimated by fitting independent liquid saturation measurements. The resulting model predicts pressure-drops very close to our measured data; its reliability with

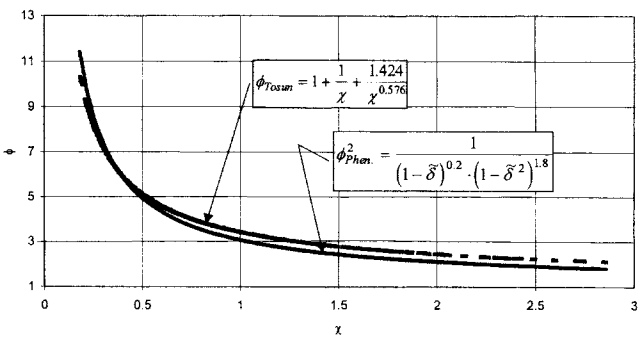

Figure 9. Comparison between the proposed model and the one by Tosun.

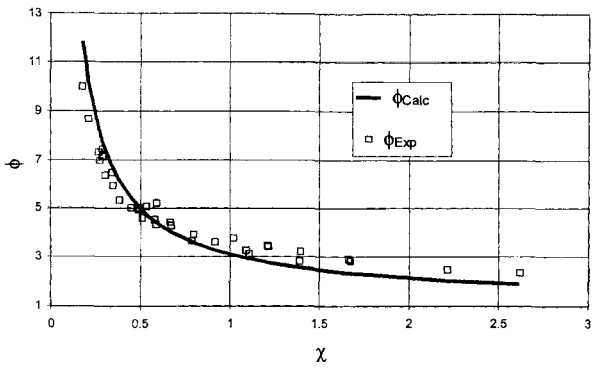

Figure 10. Extrapolation of the proposed model, Eqs. 6–7 to extrudates.

Table 10. Extrapolation of the New Model and the One by Tosun to Packing of Aluminum Extrudates

	AEa	*REa*
This work	0.125	−3.5%
Tosun	0.07	2.6%

respect to packing characteristics has been confirmed by extrapolation to yet another type of packing.

The proposed theoretical model is also in close agreement with the Tosun correlation. Thus, even if herein tested against data for an air/water system only, the model could be applicable in perspective to other kinds of fluids, too.

Experimental verification of the influence of the fluid properties, and of the operating pressure, is however in order.

Acknowledgments

The authors wish to thank Snamprogetti for financial support, and for the opportunity granted to Dario Pinna of attending his working stage.

Notation

AEa = averaged modulus of the difference between calculated and measured pressure-drops, bar/m
A_G = gas flow section, m^2
A_L = liquid flow section, m^2
a_{LG} = specific liquid-gas interfacial area per unit volume of reactor, L/m
a_{LS} = specific liquid-solid interfacial area per unit volume of reactor, m^{-1}
$d_H = 16 \cdot \epsilon^3 / (9\pi(1-\epsilon)^2)^{0.33}\, d_s$ equivalent diameter for the model of Ellman et al. (1988) and Larachi et al. (1991)
d_P = equivalent diameter of the sphere having the same volume/area ratio as the particle, m
d_s = equivalent diameter of the sphere having the same area as the particle, m
d_v = equivalent diameter of the sphere having the same volume as the particle, m
$D_e = 2/3\, d_P \cdot \epsilon(1-\epsilon)$ equivalent diameter for the model of Turpin and Huntington, m
D_G = equivalent diameter for the gas flow, m
D_L = equivalent diameter for the liquid flow, m
D_H = equivalent diameter of the interstitial channels, m
D_t = diameter of the column, m
E_1, E_2 = constants in Ergun equation
$E\ddot{o}_m = \rho_L g d_v^2 \phi_s^2 \epsilon^2 / (\sigma_L (1-\epsilon-)^2)$ Eötvos number
f_G = friction factor for gas flow over a solid
f_I = friction factor for gas flow over a liquid
f_L = friction factor for liquid flow over a solid
$f_{LG} = (\Delta P/Z)_{LG} \cdot D_e / (2\rho_G u_G^2)$, friction factor for the model of Specchia and Baldi
$f_{LG} = (\Delta P/Z)_{LG} \cdot d_H / G^2$, friction factor for the model of Ellman et al. and Larachi et al.
$Ga_L = \rho_L^2 g d_P^3 / (\mu_L^2 (1-\epsilon)^3)$ Galileo number
G = specific gas-flow rate, $kg/m^2/s$
L = specific liquid-flow rate, $kg/m^2/s$
l = coordinate along the surface of the particle, m
P = pressure, bar
Rea = averaged difference between the calculated and the measured pressure-drops, relative to the latter
$Re_G = G \cdot d_P / (\mu_G (1-,\epsilon))$ gas Reynolds number for the model of Al-Dahhan et al.
$Re_G = \rho_G \cdot v_G \cdot D_G / \mu_G$ gas Reynolds number for estimate of the friction factor f_G
$Re_L = L \cdot d_P / (\mu_L (1-\epsilon))$ liquid Reynolds number for the model of Al-Dahhan et al.
$Re'_L = \rho_L \cdot v_L \cdot D_L / \mu_L$ liquid Reynolds number for estimate of the friction factor f_L
$Re_L = L \cdot d_s / \mu_L$ liquid Reynolds number for the model of Ellman et al. (1988) and Larachi et al. (1991)
S_{LG} = liquid-gas interfacial area, m^2
S_{LS} = liquid-solid interfacial area, m^2
$t = 1/\cos\,\theta$ tortuosity of the packed bed
$u_G = G \cdot \rho_G$ gas linear velocity, m/s
$u_{G,0} = t u_G / \epsilon$ gas interstitial velocity, m/s
$u_L = L/\rho_L$ liquid linear velocity, m/s
$u_{L,0} = t u_L / \epsilon$ liquid interstitial velocity, m/s
v_G = gas actual velocity, m/s
v_L = liquid actual velocity, m/s
$We_L = L^2 d_s / (\rho_L \sigma_L)$ liquid Weber number
z = axial coordinate, m
Z = height of the bed, m

Greek letters

$\alpha = f_I / f_G$ adaptive parameter
β = liquid volume/void volume = ϵ_L/ϵ, liquid saturation
β_{stat} = static liquid volume/void volume = ϵ_{stat}/ϵ, static liquid saturation
δ = equivalent diameter of the gas channel, m
ϵ = void volume/reactor volume, packing void fraction
ϵ_G = gas volume/reactor volume = gas holdup
ϵ_L = liquid volume/reactor volume liquid holdup
$\xi = (Re_G)^{1.167} / (Re_L)^{0.767}$ Turpin and Huntington parameter
θ = average settlement angle of the particles
$\kappa = X_G\, (Re_L We L)^{0.25}$ parameter for the model of Larachi et al.
μ_G = gas viscosity, kg/m/s
μ_L = liquid viscosity, kg/m/s
$\xi = (Re_L^{0.25} We_L^{0.2}) / ((1 + 3.17 Re_L^{1.65} We_L^{1.2})^{0.1})$ parameter for the model of Ellman et al.
ρ_G = gas density, kg/m^3
ρ_L = liquid density, kg/m^3
σ_L = liquid surface tension, kg/s^2
τ_{LG} = friction at the liquid-gas interface, bar
τ_{LS} = friction at the liquid-solid interface, bar
$\phi_s = d_P / d_v$ sphericity factor of bed packing
$\phi = ((\Delta P/Z)_{LG} / (\Delta P/Z)_L)^{0.5}$ second Lockhart-Martinelli parameter
$\chi = ((\Delta P/Z)_L (\Delta P/Z)_G)^{0.5}$ first Lockhart-Martinelli parameter
$\chi_G = G/L (\rho_L/\rho_G)^{0.5}$ modified gas Lockhart-Martinelli parameter
$\chi_L = L/G (\rho_G/\rho_L)^{0.5}$ modified liquid Lockhart-Martinelli parameter
$\psi = \sigma_W/\sigma_L [\mu_L/\mu_W (\rho_W/\rho_L)^2]^{1/3}$ Charpentier and Favier parameter
$\Delta P/Z$ = average pressure drop across the reactor, bar/m
$\Psi_L = 1/\rho_L g ((\Delta P/Z)_{LG} + \rho_L g)$ dimensionless pressure-drop
$\Psi_G = 1/\rho_G g ((\Delta P/Z)_{LG} + \rho_G g)$ dimensionless pressure-drop

Subscripts

0 = single-phase flow
Calc = calculated

Exp = experimental
G = gas
i = ith experiment
I = interfacial area
L = liquid
LG = two-phase flow
Meas = measured
OUT = column outlet
Phen = phenomenological
R = reactor
ref = reference
W = water

Literature Cited

Al-Dahhan, M. H., M. R. Khadilkar, Y. Wu, and M. P. Dudukovic, "Prediction of Pressure Drop and Liquid Holdup in High-Pressure Trickle-Bed Reactors," *Ind. Eng. Chem. Res.* **37**, 793 (1998).

Audibert, F., A. Suger, and H. Van Landeghem, U.S. Patent 4,413,063 (1983).

Benkird, K., S. Rode, and N. Midoux, "Prediction of Pressure Drop and Liquid Saturation in Trickle-Bed Reactors Operated in High Interaction Regimes," *Chem. Eng. Sci.*, **52**, 4021 (1997).

Bensetiti, Z., F. Larachi, B. P. A. Grandjean, and G. Wild, "Liquid Saturation in Cocurrent Upflow Fixed-Bed Reactors: a State of the Art Correlation," *Chem. Eng. Sci.*, **52**, 4239 (1997).

Bird, R. B., W. E. Stewart, and E. N. Lightfoot, *Transport Phenomena*, Wiley, New York (1960).

Buzzi-Ferraris, G., *Metodi numerici e software in C++*, Addison Wesley, Milano (1998).

Charpentier, J. C., "Étude de la Rétention de Liquide dans une Colonne à Garnissage Arrosé à Co-Courant et à Contre-Courant de Gaz-Liquide. Représentation de sa Texture par un Modèle à Films, Filets et Gouttes," *Chemie et Industrie-Genie Chimique*, **99**, 803 (1968).

Charpentier, J. C. and M. Favier, "Some Liquid Holdup Experimental Data in Trickle-Bed Reactors for Foaming and Non-Foaming Hydrocarbons," *AIChE J.*, **21**, 1213 (1975).

Charpentier, J. C., "Recent Progress in Two-Phase Gas-Liquid Mass Transfer in Packed Beds," *Chem. Eng. J.*, **11**, 161 (1976).

Charpentier, J. C., "Hydrodynamics of Two-Phase Flow Through Porous Media," *J. Powd. Bulk Sol. Techn.*, **2**, 68 (1978).

Chaumette, P., P. Boucot, and P. H. Galtier, EP Patent 0, 753, 562, A1 (1996).

Cybulski, A., R. Edvinsonn, S. Irandoust, and B. Andersson, "Liquid-Phase Methanol Synthesis: Modelling of a Monolithic Reactor," *Chem. Eng. Sci.*, **43**, 3463 (1993).

Cybulski, A., "Liquid-Phase Methanol Synthesis: Catalyst, Mechanism, Kinetics, Chemical Equilibria, Vapor-Liquid Equilibria, and Modeling-A Review," *Catal. Rev.-Sci. Eng.*, **36**, 557 (1994).

Dudukovic, M. P. P., and L. Mills, *Encyclopedia of Fluid Mechanics*, Chap. 32, Gulf publishing, Houston (1986).

Ellman, M. J., N. Midoux, A. Laurent, J. C. Charpentier, "A New Improved Pressure Drop Correlation for Trickle-Bed Reactors," *Chem. Eng. Sci.*, 43, **8**, 2201 (1988).

Galtier, P., A. Forestière, and P. Trambouze, "Modeling of Methanol Synthesis in a Three-Phase Fixed-Bed Reactor," *Chem. Eng. Sci.*, **41**, 973 (1986).

Hicks, R. E., "Pressure Drop in Packed Beds of Spheres," *Ind. Eng. Chem. Fundam.* **9**, 500, (1970).

Holub, R. A., M. P. Dudukovic, and A. Ramachandran, "A Phenomenological Model for Pressure Drop, Liquid Holdup and Flow Regime Transition in Gas-Liquid Trickle-Flow," *Chem. Eng. Sci.*, **47**, 2343 (1992).

Holub, R. A., M. P. Dudukovic, and A. Ramachandran, "Pressure Drop, Liquid Holdup and Flow Regime Transition in Trickle-Flow," *AIChE J.*, **39**, 302 (1993).

Kodra, D., and J. Levec, "Liquid Phase Methanol Synthesis: Comparison Between Trickle-Bed and Bubble Column Slurry Reactors," *Chem. Eng. Sci.*, **46**, 2339 (1991).

Lamine, A. S., L. Gerth, H. Le Gall, G. Wild, "Heat Transfer in a Packed Bed Reactor with Cocurrent Downflow of a Gas and a Liquid," *Chem. Eng. Sci.*, **51**, 3813 (1996).

Larachi, F., A. Laurent, N. Midoux, and G. Wild, "Experimental Study of Trickle-Bed Reactor Operating at High Pressure: Two-Phase Pressure Drop and Liquid Saturation," *Chem. Eng. Sci.*, **46**, 1233 (1991).

Lockhart, R. W., and R. C. Martinelli, "Proposed Correlation of Data for Isothermal Two-Phase, Two Component Flow in Pipe," *Chem. Eng. Prog.*, **45**, 39 (1949).

Maers, D. E., "Test for Transport Limitations in Experimental Catalytic Reactors," *Ind. Eng. Chem. Proc. Des. Dev.*, **10**, 541 (1971).

Morsi, B. I., A. Laurent, N. Midoux, G. Barthole-Delauney, A. Storck, and J. C. Charpentier, "Hydrodynamics and Gas-Liquid Interfacial Parameters of Concurrent Downward Two-Phase Flow in Trickle Bed Reactors," *Chem. Eng. Commun.*, **25**, 267 (1984).

Paraskos, J. A., J. A. Frayer, and Y. T. Shah, "Effect of Holdup in Complete Catalyst Wetting and Backmixing During Hydroprocessing in Trickle-Bed Reactors," *Ind. Eng. Chem. Proc. Des. Dev.*, **14**, 315 (1975).

Pass, G., C. Holzhauser, A. Akgerman, and R. G. Anthony, "Methanol Synthesis in a Trickle-Bed Reactor," *AIChE J.*, **36**, 1054 (1990).

Perry, R. H., and D. Green, *Chemical Engineer's Handbook*, 6th ed., McGraw-Hill, New York (1984).

Pinna, D., "Fluidodinamica di Reattori Trickle-Bed Operanti in Regime ad Elevata Interazione," Thesis in Chemical Engineering, Politecnico di Milano, (1999).

Rode, S., N. Midoux, M. A. Latifi, A. Storck, "Hydrodynamics and Liquid-Solid Mass Transfer Mechanism in Packed Beds Operating in Cocurrent Gas-Liquid Downflow: an Experimental Study Using Electrochemical Shear Rate Sensors," *Chem. Eng. Sci.*, **49**, 1383 (1994).

Saez, E., and R. G. Carbonell, "Hydrodynamic Parameters for Gas-Liquid Cocurrent Flow in Packed Beds," *AIChE J.*, **31**, 52 (1985).

Satterfield, C., "Trickle-Bed Reactors," *AIChE J.*, **21**, 209 (1975).

Satterfield, C., and P. F. Way, "The Role of the Liquid Phase in the Performance of a Trickle-Bed Reactor," *AIChE J.*, **18**, 305 (1972).

Specchia, V., and G. Baldi, "Pressure Drop and Liquid Holdup for Two Phase Concurrent Flow in Packed Beds," *Chem. Eng. Sci.*, **32**, 515 (1977).

Taitel, Y., and A. E. Dukler, "A Theoretical Approach to the Lockhart-Martinelli Correlation for Stratified Flow," *Int. J. Multiphase Flow*, **2**, 591 (1976).

Tjandra, S., R. G. Anthony, and A. Akgerman, "Low H_2/CO Ratio Synthesis Gas Conversion to Methanol in a Trickle-Bed Reactor," *Ind. Eng. Chem. Res.*, **32**, 2602 (1993).

Tosun, G., "A Study of Cocurrent Downflow of Nonfoaming Gas-Liquid Systems in a Packed Bed. 1. Flow Regimes: Search of a Generalized Flow Map; 2. Pressure Drop: Search for a Correlation," *Ind. Eng. Chem. Proces Des. Dev.*, **23**, 35 (1984).

Turpin, J., L., and R. L. Huntington, "Prediction of Pressure Drop for Two-Phase, Two Component Concurrent Flow in Packed Beds," *AIChE J.*, **13**, 1196 (1967).

Ullman's Encyclopedia of Industrial Chemistry, Vol. A16, 5th Ed. Barbara Elvers, Stephen Hawking, Gail Schultz, eds., Weinheim, Germany (1990).

Yang, X. L., G. Wild, and J. P. Euzen, "Study of Liquid Retention in Fixed-Bed Reactors with Upward Flow of Gas and Liquid," *Int. Chem. Eng.*, **33**, 2 (1993).

Wammes, W. J. A., J. Middelkamp, W. J. Huisman, C. M. deBaas, and K. R. Westerterp, "Hydrodynamics in a Cocurrent Gas-Liquid Trickle-Bed at Elevated Pressures," *AIChE J.*, **37**, 1849 (1991).

Appendix: Derivation of the Lockhart-Martinelli-Type Model for Pressure Drop and Liquid Saturation in High Interaction Regime TBRs

The momentum balances on the two phases are two steady-state equilibrium equations involving the shear forces at the liquid-solid and gas-liquid interfaces and the force due to pressure drop across the bed

$$\epsilon\beta \cdot \frac{dP}{dl} = \tau_{LS} a_{LS} - \tau_{LG} a_{LG} \quad \text{liquid phase} \qquad \text{(A1)}$$

$$\epsilon(1-\beta)\cdot\frac{dP}{dl}=\tau_{LG}a_{LG}\quad\text{gas phase}\tag{A2}$$

In order to write Eqs. A1 and A 2 in a dimensionless form, the geometry shown in Figure 6 is assumed: the liquid and the gas are supposed to flow through a channel, representative of the void interstices between the solid particles. The channel has an equivalent diameter D_H and forms an angle θ with the vertical axis.

This leads to define the tortuosity t as

$$t=\frac{1}{\cos\vartheta}\tag{A3}$$

The flow is assumed to be annular, the gas moving through a channel of diameter δ.

Given these premises, all the geometrical variables of the system can be expressed in terms of the equivalent diameter D_H and the dimensionless parameter $\tilde{\delta}$

$$\tilde{\delta}=\frac{\delta}{D_H}\tag{A4}$$

Also, the liquid saturation being

$$\beta=1-\tilde{\delta}^2\tag{A5}$$

Equations A1 and A2 can be rewritten as follows

$$(1-\tilde{\delta}^2)\cdot\frac{dP}{dz}=t\frac{4}{D_H}\left(\tau_{LS}-\tau_{LG}\tilde{\delta}\right)\tag{A6}$$

$$\tilde{\delta}^2\cdot\frac{dP}{dz}=t\frac{4}{D_H}\tau_{LG}\tilde{\delta}\tag{A7}$$

The shear forces can be related to friction factors at the interfaces

$$\tau_{LS}=f_L\cdot\frac{1}{2}\rho_L v_L^2\tag{A8}$$

$$\tau_{LG}=f_I\cdot\frac{1}{2}\rho_G(v_G-v_L)^2\cong f_I\cdot\frac{1}{2}\rho_G v_G^2\tag{A9}$$

On introducing dimensionless velocities as the ratio of the real velocities to the interstitial ones

$$\tilde{u}_L=\frac{v_L}{u_{L,0}}\tag{A10}$$

$$\tilde{u}_G=\frac{v_G}{u_{G,0}}\tag{A11}$$

substituting Eqs. A8, A9, A10 and A11 into Eqs. A6 and A7, and eliminating dP/dz between Eq. A6 and A7, we get

$$\frac{1-\tilde{\delta}^2}{\tilde{\delta}}=\frac{f_L\dfrac{\rho_L u_{L,0}^2}{2}}{f_I\dfrac{\rho_G u_{G,0}^2}{2}}\frac{\tilde{u}_L^2}{\tilde{u}_G^2}-\tilde{\delta}\tag{A12}$$

If f_I is assumed to be proportional to f_G by a factor α, both the friction factors f_I and f_L can be estimated using the equations

$$f_L=C\cdot(Re'_L)^{-0.2}\tag{A13}$$

$$f_I=\alpha\cdot f_G=\alpha\cdot C\cdot(Re'_G)^{-0.2}\tag{A14}$$

where C is a constant.

It can be shown that if the Reynolds numbers present in Eqs. A13 and A14 are calculated with the real velocity and with the equivalent diameters for the two phases, the above expressions correspond to the Hicks equation for friciton factor in packed beds (Hicks, 1970).

So Equations A13 and A14 lead to:

$$f_L=C\left(\frac{\rho_L v_L D_H(1-\tilde{\delta})}{\mu_L}\right)^{-0.2}$$

$$=C\left(\frac{\rho_L u_{L,0}D_H}{\mu_L}\right)^{-0.2}\left[\tilde{u}_L(1-\tilde{\delta})\right]^{-0.2}=f_{L,0}\left[\tilde{u}_L(1-\tilde{\delta})\right]^{-0.2}\tag{A15}$$

$$f_I=\alpha\cdot C\left(\frac{\rho_G v_G D_H\tilde{\delta}}{\mu_G}\right)^{-0.2}$$

$$=\alpha\cdot C\left(\frac{\rho_G u_{G,0}D_H}{\mu_G}\right)^{-0.2}\left(\tilde{u}_G\tilde{\delta}\right)^{-0.2}=\alpha\cdot f_{G,0}\left(\tilde{u}_G\tilde{\delta}\right)^{-0.2}\tag{A16}$$

where $f_{L,0}$ and $f_{G,0}$ are the friction factors for single phase flow through the channel.

Now since

$$f_{L,0}\frac{\rho_L u_{L,0}^2}{2}=\left(\frac{dP}{dl}\right)_L\frac{D_H}{4}=\frac{1}{t}\left(\frac{dP}{dz}\right)_L\frac{D_H}{4}\tag{A17}$$

$$f_{G,0}\frac{\rho_G u_{G,0}^2}{2}=\left(\frac{dP}{dl}\right)_G\frac{D_H}{4}=\frac{1}{t}\left(\frac{dP}{dz}\right)_G\frac{D_H}{4}\tag{A18}$$

Equation A12 can be restated as follows

$$\frac{1-\tilde{\delta}^2}{\tilde{\delta}}=\frac{f_{L,0}\dfrac{\rho_L u_{L,0}^2}{2}}{\alpha\cdot f_{G,0}\dfrac{\rho_G u_{G,0}^2}{2}}\left(\frac{1-\tilde{\delta}}{\tilde{\delta}}\frac{\tilde{u}_L}{\tilde{u}_G}\right)^{-0.2}\frac{\tilde{u}_L^2}{\tilde{u}_G^2}-\tilde{\delta}$$

$$=\frac{\left(\dfrac{dP}{dz}\right)_L}{\alpha\cdot\left(\dfrac{dP}{dz}\right)_G}\left(\frac{1-\tilde{\delta}}{\tilde{\delta}}\right)^{-0.2}\left(\frac{\tilde{u}_L}{\tilde{u}_G}\right)^{1.8}-\tilde{\delta}\tag{A19}$$

which provides a relationship between the two-phase pressure-drop, the single-phase pressure-drops, the dimensionless parameter $\tilde{\delta}$ and the dimensionless velocities $\tilde{u}_L$ and $\tilde{u}_G$.

On introducing the dimensionless Lockhart-Martinelli parameter

$$\chi = \sqrt{\frac{\left(\frac{dP}{dz}\right)_L}{\left(\frac{dP}{dz}\right)_G}} \tag{A20}$$

Eq. A19 becomes:

$$\chi^2 = \alpha \cdot \frac{(1-\tilde{\delta})^{0.2}}{\tilde{\delta}^{1.2}} \left(\frac{\tilde{u}_G}{\tilde{u}_L}\right)^{1.8} \tag{A21}$$

Similarly, using Eqs. A8, A9, A10, A11, A15, A16, A17 and A18, Eq. A6 can be rearranged into

$$\frac{1}{t}(1-\tilde{\delta}^2)\cdot\frac{dP}{dz} = f_{L,0}\frac{\rho_L u_{L,0}^2}{2}\cdot\frac{4}{D_H}\cdot(1-\tilde{\delta})^{-0.2}\tilde{u}_L^{-0.2}\cdot\tilde{u}_L^2 - \alpha\cdot f_{G,0}\frac{\rho_G u_{G,0}^2}{2}\cdot\frac{4}{D_H}\cdot\tilde{\delta}^{-0.2}\tilde{u}_G^{-0.2}\tilde{u}_G^2\tilde{\delta} \tag{A22}$$

that is

$$(1-\tilde{\delta}^2)\cdot\frac{dP}{dz} = \left(\frac{dP}{dz}\right)_L\cdot(1-\tilde{\delta})^{-0.2}\cdot\tilde{u}_L^{1.8} - \alpha\cdot\left(\frac{dP}{dz}\right)_G\cdot\tilde{u}_G^{1.8}\tilde{\delta}^{0.8} \tag{A23}$$

Defining the second Lockhart-Martinelli parameter ϕ as

$$\phi = \sqrt{\frac{\frac{dP}{dZ}}{\left(\frac{dP}{dZ}\right)_L}} \tag{A24}$$

Eq. A23 leads to

$$\phi^2 = \frac{1}{1-\tilde{\delta}^2}\left((1-\tilde{\delta})^{-0.2}\tilde{u}_L^{1.8} - \alpha\cdot\frac{\tilde{\delta}^{0.8}}{\chi^2}\cdot\tilde{u}_G^{1.8}\right). \tag{A25}$$

Combining Eqs. A 21 and A25.

$$\phi^2 = \frac{1}{(1-\tilde{\delta})^{0.2}}\tilde{u}_L^{1.8} \tag{A26}$$

The dimensionless velocities can be expressed as functions of $\tilde{\delta}$

$$\nu_L = \frac{tu_L}{\epsilon\beta} = \frac{u_{L,0}}{\beta} \Rightarrow \tilde{u}_L = \frac{\nu_L}{u_{L,0}} = \frac{1}{\beta} = \frac{1}{1-\tilde{\delta}^2} \tag{A27}$$

$$\nu_G = \frac{tu_G}{\epsilon(1-\beta)} = \frac{u_{G,0}}{1-\beta} \Rightarrow \tilde{u}_G = \frac{\nu_G}{u_{G,0}} = \frac{1}{1-\beta} = \frac{1}{\tilde{\delta}^2} \tag{A28}$$

Eventually, introducing Eqs. A27 and A28 into Eqs. A21 and A26 we get the final expression of the model, which represents a relationship between single-phase pressure-drops, two-phase pressure-drop and liquid saturation through the definition of the Lockhart-Martinelli parameters and the equivalent dimensionless diameter of the gas channel $\tilde{\delta}$.

$$\chi^2 = \alpha\cdot\frac{(1-\tilde{\delta})^{0.2}(1-\tilde{\delta}^2)^{1.8}}{\tilde{\delta}^{4.8}} \tag{A29}$$

$$\delta^2 = \frac{1}{(1-\tilde{\delta})^{0.2}\cdot(1-\tilde{\delta}^2)^{1.8}} \tag{A30}$$

Equations A29 and A30 correspond to Eqs. 6 and 7 in the main text.

Finally, it can be easily demonstrated that even when the geometry of the system is slightly different from the one described in Figure 6, the proposed model remains valid. In fact, upon introducing a correction factor k for the real gas-liquid interfacial area, referred to the annular description

$$k = \frac{dS_{LG}^{\text{real}}}{dS_{LG}^{\text{annular}}} \tag{A31}$$

the momentum balance equations result in the same final expression linking the Lockhart-Martinelli parameters A29 and A30, provided that α is replaced by $\alpha\cdot k$.

Manuscript received May 17, 1999, and revision received Oct. 4, 1999.